FEMS Microbiology Ecology, 93, 2017, fix053

doi: 10.1093/femsec/fix053
Advance Access Publication Date: 25 April 2017
Research Article

RESEARCH ARTICLE

Polyphosphate-accumulating bacterial community colonizing the calcium bodies of terrestrial isopod crustaceans *Titanethes albus* and *Hyloniscus riparius*

Rok Kostanjšek[1,*], Miloš Vittori[1], Vesna Srot[2], Peter A. van Aken[2] and Jasna Štrus[1]

[1]Department of Biology, Biotechnical Faculty, University of Ljubljana, Jamnikarjeva 101, SI-1000 Ljubljana, Slovenia and [2]Stuttgart Center for Electron Microscopy, Max Planck Institute for Solid State Research, Heisenbergstrasse 3, 70569 Stuttgart, Germany

[*]**Corresponding author:** Department of Biology, Biotechnical Faculty, University of Ljubljana, Jamnikarjeva 101, SI-1000 Ljubljana, Slovenia. Tel: +386-1-320-33-73; Fax: +386-1-257-33-90; E-mail: rok.kostanjsek@bf.uni-lj.si

One sentence summary: The manuscript presents the first evidence of polyphosphate-accumulating bacterial community associated with the tissue of a terrestrial animal described in the calcium bodies—specialized organs for calcium storage in terrestrial isopod crustaceans.

Editor: Rolf Kümmerli

ABSTRACT

Terrestrial isopods from the group Trichoniscidae accumulate calcium in specialized organs, known as the calcium bodies. These consist of two pairs of epithelial sacs located alongside the digestive system. These organs contain various forms of calcium and constantly present bacteria. To elucidate their origin and role, we analyzed the bacteria of the calcium bodies in the cave-dwelling isopod *Titanethes albus* and the epigean species *Hyloniscus riparius*, by microscopy, histochemistry, energy dispersive X-ray spectrometry, 16S rRNA analysis and *in situ* hybridization. The calcium bodies of both species comprise numerous and diverse bacterial communities consisting of known soil bacteria. Despite their diversity, these bacteria share the polyphosphate-accumulation ability. We present the model of phosphorous dynamics in the calcium bodies during the molting cycle and potentially beneficial utilization of the symbiotic phosphate by the host in cyclic regeneration of the cuticle. Although not fully understood, this unique symbiosis represents the first evidence of polyphosphate-accumulating bacterial symbionts in the tissue of a terrestrial animal.

Keywords: arthropods; bacteria; symbiosis; polyphosphate

INTRODUCTION

Terrestrial isopods (Isopoda, Oniscidea), commonly known as sowbugs, woodlice, pillbugs and slaters, are the most diverse group of crustaceans inhabiting terrestrial environments. Their successful transition to a terrestrial way of life (Warburg 1987; Hornung 2011) includes metabolic pathways for maintenance of calcium homeostasis, which is essential for exoskeleton mineralization. To minimize the loss of this element during frequent molting of their cuticle, terrestrial isopods have developed several mechanisms of calcium resorption from the old cuticle prior to exuviation, transitional storage of the calcium in specialized organs or tissues and its incorporation into the newly formed cuticle. Most commonly, the calcium is stored as sternal $CaCO_3$ deposits (Ziegler 2005; Ziegler, Fabritius and Hagedorn 2005), which form during premolt in the space between the detached old cuticle and epithelium of the first four

Received: 25 December 2016; **Accepted:** 17 April 2017

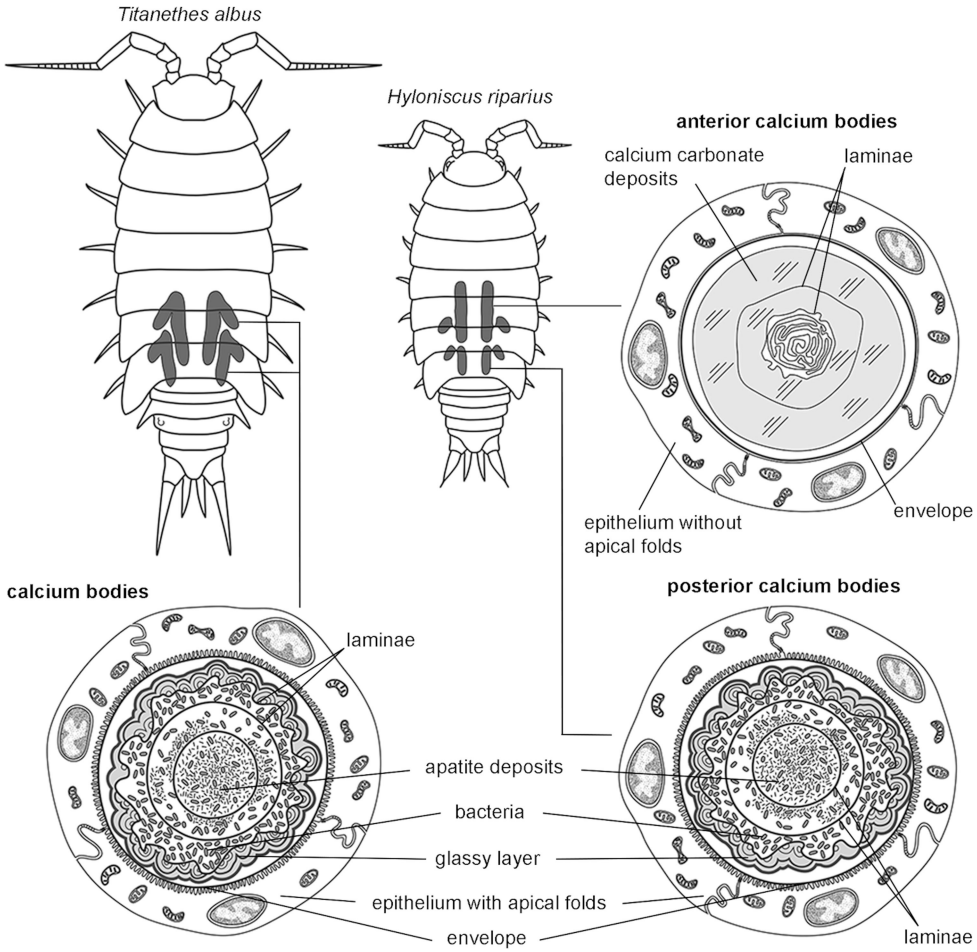

Figure 1. Position of the calcium bodies. A diagrammatic representation of the position of calcium bodies in the large subterranean trichoniscid *T. albus* (left) and the smaller epigean species *H. riparius* (right). Both species possess two pairs of calcium bodies. In *T. albus*, both pairs contain bacteria and calcium phosphate concretions and are delimited by an epithelium with prominent apical folds. In *H. riparius*, the posterior pair of calcium bodies is similar to the calcium bodies of *T. albus*, whereas the anterior pair is devoid of bacteria, contains $CaCO_3$ and is delimited by an epithelium lacking apical folds.

anterior body segments (Ziegler 1997, 2007; Becker *et al.* 2003; Ziegler, Fabritius and Hagedorn 2005). In addition, terrestrial isopods from the group Trichoniscidae accumulate calcium in specialized organs, known as the calcium bodies (Vittori *et al.* 2012). These consist of two pairs of epithelial sacs and are located in the body cavity, alongside the digestive system (Méhelÿ 1932) (Fig. 1).

Microscopic anatomy studies of the calcium bodies in the cave isopod *Titanethes albus* (Vittori *et al.* 2012) and the much smaller epigean species *Hyloniscus riparius* showed a continuous monolayered epithelium surrounding the contents of the organ, comprising abundant bacteria and calcified matrix. The calcified matrix appears as an amorphous 'glassy' layer, just below the epithelium, or as mineralized concretions in the core of the calcium body. While the latter comprises calcium phosphate in the stable form of apatite, the dynamic glassy layer contains mainly calcium carbonate and lesser amounts of phosphorus (Vittori *et al.* 2012). The dynamics of the glassy layer includes constant formation and reabsorption of materials during the molting cycle, indicating its role in transitional storage of calcium, while the mineralized core remains more or less unchanged (Vittori *et al.* 2012). A dense bacterial population colonizes the area between the glassy layer and the core of calcium bodies. Bacterial formations are arranged in concentric layers separated by thin laminae, while the mineralized core includes individual bacteria embedded in the apatite matrix. Observations of *T. albus* (Vittori *et al.* 2012), *H. riparius* and other isopod species, such as *Androniscus roseus* and *Haplophthalmus mengii* (Vittori and Štrus 2016), strongly suggest that the bacterial presence in the calcium bodies is a general feature of trichoniscids. In contrast, the anterior pair of the calcium bodies of *H. riparius* is devoid of bacteria and contains only concentric layers of calcium carbonate, while the posterior pair is filled with bacteria-containing matrix mineralized with apatite (Vittori *et al.* 2013), as in other trichoniscids (Fig. 1).

Bacteria and terrestrial isopods established a wide array of associations, ranging from facultative transients to highly adapted symbionts (reviewed in Bouchon, Zimmer and Dittmer 2016). The latter includes sex-ratio distorting *Wolbachia* (Dittmer *et al.* 2014), pathogenic *Rhabdochlamydia porcellionis* (Kostanjsek *et al.* 2004), *Rickettsiella armadillidii* (Cordaux *et al.* 2007) and '*Candidatus* Hepatincola porcellionum' (Wang *et al.* 2004b), commensalistic '*Candidatus* Bacilloplasma' (Kostanjsek, Strus and Avgustin 2007) and presumably mutualistic 'Candidatus *Hepatoplasma crinochetorum*' (Fraune and Zimmer 2008; Wang *et al.* 2004a). In addition, a considerable diversity of ubiquitous bacteria has been detected in all major tissues of terrestrial isopods (Dittmer *et al.* 2016). Their highest diversity has been observed in

the digestive system (Kostanjšek *et al.* 2006; Dittmer *et al.* 2016; Horvathova, Babik and Bauchinger 2016), where bacteria can be utilized as an additional source of nutrients and digestive enzymes (Zimmer 2002). Although their role in the isopod's digestive system is far from being fully understood, these bacteria facilitate the growth and increase the survival rate of the isopods (Horvathova, Kozlowski and Bauchinger 2015). A surprising diversity of ubiquitous bacteria have also been described in several other tissues of isopod *Armadillidium vulgare*, indicating their ability to occupy various niches within isopod (Bouchon, Zimmer and Dittmer 2016; Dittmer *et al.* 2016). In this view, the association of these bacteria with the host is most likely commensalistic or opportunistic (Bouchon, Zimmer and Dittmer 2016).

Common presence and large numbers of bacteria inhabiting the confined sacs of calcium bodies without any obvious signs of pathogenesis for the trichoniscid hosts (Vittori *et al.* 2012, 2013) suggest adaptation and balance between the host and the symbionts. In order to elucidate the nature of this association and the potential symbiotic role of the bacteria in the calcium bodies, we analyzed these bacteria in two trichoniscid species, the cave dwelling *T. albus* and the epigean *H. riparius*, with a combination of electron microscopy, histochemistry, energy dispersive X-ray spectrometry (EDXS), 16S rRNA gene sequence analysis and *in situ* hybridization.

MATERIAL AND METHODS

Isopod material

Adult individuals of *Titanethes albus* were collected from Planina cave in central Slovenia and transferred into the laboratory, where their calcium bodies were dissected under sterile conditions the same day. Adult *Hyloniscus riparius* individuals were sampled near Ormož in northeastern Slovenia and kept on substrate and leaf litter from the sampling site until dissection of their calcium bodies.

DNA extraction, PCR, cloning, and sequencing

The calcium bodies from two *T. albus* and two *H. riparius* individuals were isolated under sterile conditions. Four separate samples of genomic DNA, each containing the genetic material of the calcium bodies from one individual, were obtained by the QIAmp DNA Mini Kit (Qiagen, Valencia, CA). Bacterial 16S rRNA genes from each sample were amplified in four separate polymerase chain reactions (PCRs) as described previously (Kostanjsek *et al.* 2013), by using the bacteria-specific primers 27F and 1492R. The same PCR protocol was used in attempts of archaeal 16S rRNA gene amplification from the same samples by using the primers Arch21F and Arch958R (DeLong 1992). PCR products of the expected size were purified and cloned by Macrogen cloning service (Amsterdam, the Netherlands). Four clone libraries from the calcium bodies of two *T. albus* individuals (named Ta1 and Ta2) and two *H. riparius* individuals (named Hr1 and Hr2) were constructed from randomly selected clones of each sample and sequenced using the 27F and 1492R primers, by the Macrogen sequencing service (Amsterdam, the Netherlands).

Sequence analysis

Obtained sequences were assembled and edited by ChromasPro software ver. 1.6 (Technelysium Pty Ltd, South Brisbane, Australia). Putative chimeric sequences identified by DECIPHER (Wright, Yilmaz and Noguera 2012) were omitted from the study. The sequences were aligned by Muscle multiple alignment software version 3.8.31 (Edgar 2004) and checked manually for ambiguous nucleotides. Assembled and edited sequences were compared to sequences deposited in RDP (http://rdp.cme.msu.edu/) by using SEQUENCE MATCH tool (Cole *et al.* 2014).

Sequences from each clone library were assigned to operational taxonomic units (OTUs) at an evolutionary distance of 0.01 (Kim *et al.* 2014) by a clustering approach implemented in MOTHUR (Schloss *et al.* 2009).

The sequences obtained in this study were deposited in GenBank under accession numbers KU533909–KU534080.

Sample preparation and microscopy investigations

For scanning electron microscopy (SEM), isolated calcium bodies from five specimens of each species were fixed in 2.5% glutaraldehyde and 2% formaldehyde in 0.1 M cacodylate buffer, pH = 7.3 at 4°C overnight. After washing of the fixative with 0.1 M cacodylate buffer, the samples were postfixed in 1% aqueous OsO_4 for 1 h. They were then dehydrated in an ascending ethanol series, after which ethanol was substituted with pure acetone. Samples were then air-dried in hexamethyldisilazane. Dry samples were attached to metal holders with silver paint and fractured to expose the interior. Specimens were coated with platinum and observed with a JEOL JSM-7500F (JEOL, Tokio, Japan) field-emission scanning electron microscope.

For light microscopy, three specimens of each species were used. Posterior parts of the bodies containing calcium bodies were fixed in 4% formaldehyde for 4 h at 4°C, washed and decalcified in 10% ethylene-diamine-tetra-acetic acid for 4 h. Samples were dehydrated in an ethanol series, cleared in xylene and embedded in paraffin. Tissue sections (7 μm) were cut on a rotary microtome, transferred onto glass slides, deparaffinized with xylene and rehydrated in a descending ethanol series. For histochemical detection of polyphosphates (polyP) (Ascher-Sobbi *et al.* 2008), tissue sections were stained with aqueous 4′,6-diamidino-2-phenylindole (DAPI) solution in concentration of 10 μg/mL (Günther *et al.* 2009). After 60-min incubation in the dark and at room temperature, sections were observed under filter set 01 (Zeiss, Oberkochen, Germany) (365/12 nm excitation, 397 nm emission) and observed with an Axioimager Z.1 microscope using an ApoTome system (Zeiss, Oberkochen, Germany) for structured illumination.

For ultrastructural observation of bacteria with transmission electron microscopy (TEM), the calcium bodies from three specimens of each species were fixed as described for SEM, dehydrated in an ascending ethanol series and embedded in Spurr's resin (SPI, West Chester, PA). Ultrathin sections were contrasted with uranyl acetate and lead citrate and observed with a CM 100 transmission electron microscope (Philips, Eindhoven, The Netherlands).

Fluorescence *in situ* hybridization

The hybridization was performed on tissues sections prepared as described above and under previously described conditions (Daims, Stoecker and Wagner 2005). The applied rRNA-targeted probes and formamide concentrations are listed in Table 1. In addition to a previously published probe used as negative control (NON-338) (Wallner, Amann and Beisker 1993) and class-specific probes for Betaproteobacteria (BET42a) (Manz *et al.* 1992)

Table 1. Oligonucleotide probes used in this study.

Probe	Sequence (5′–3′)	Target site (*Escherichia coli* numbering)	% Formamide	Target group	Reference
Alph-968	GGTAAGGTTCTGCGCGTT	16S, 968–985	20%	Alphaproteobacteria except Rickettsiales	Neef (1997)
BET42a	GCCTTCCCACTTCGTTT	23S, 1027–1043	35%	Betaproteobacteria—partial	Manz *et al.* (1992)
S-O-Bac-0962-a-A-19	GTAAGGTTCCTCGCGTATC	16S, 962–980	20%	Bacteroidetes—partial	This study
NON338	ACTCCTACGGGAGGCAGC	16S	35%	Negative control probe	Wallner *et al.* (1993)

Table 2. Results of sequencing of representative 16S rRNA gene clones.

OTU[a] (no. of sequences)	Accession number	The highest match in RDP database [accession number]	% of shared nucleotide 7-mers (S_ab score)	Class and order according to RDP
Ta1-1 (51)	KU534024	*Chitinophaga soli* Gsoil 219 [NR112622]	0.929	Bacteroidetes/Chitinophagales
Ta1-16 (27)	KU534031	*Aminobacter anthyllidis* STM4645 [NR108530]	0.941	Alphaproteobacteria/Rhizobiales
Ta1-17 (9)	KU533992	*Sphingopyxis bauzanensis* BZ30 [NR117213]	0.942	Alphaproteobacteria/Sphingomonadales
Ta2-1 (8)	KU534061	*Rhizobium* sp. MN6-12 [JQ396566]	0.951	Alphaproteobacteria/Rhizobiales
Ta1-6 (6)	KU534015	U.C.[b] clone AK1DE2_01H [GQ397005]	0.878	Alphaproteobacteria/Bradyrhizobiales
Ta1-2 (4)	KU534033	*Mesorhizobium chacoense* PR5 [NR025411]	0.896	Alphaproteobacteria/Rhizobiales
Ta2-8 (4)	KU534021	U.C.[b] *Devosia* sp. clone O:RM-A3 [HE974822]	0.919	Alphaproteobacteria/Rhizobiales
Ta2-27 (3)	KU534014	*Mesorhizobium amorphae* JN37 [KF150349]	0.916	Alphaproteobacteria/Rhizobiales
Hr1-5 (26)	KU533950	*Variovorax paradoxus* EPS [NR074646]	0.946	Betaproteobacteria/Burkholderiales
Hr1-1 (18)	KU533935	*Sphingobacterium multivorum* [AB680731]	0.925	Bacteroidetes/Sphingobacteriales
Hr1-2 (13)	KU533946	U.C.[b] *Mesorhizobium* sp. clone 4h-64 [FJ444740]	0.861	Alphaproteobacteria/Rhizobiales
Hr2-8 (3)	KU533983	U.C.[b] clone 3BR-3BB 16S [EU937880]	0.895	Bacteroidetes/Chitinophagales

[a]named after representing clone.
[b]U.C.—uncultured.

and Alphaproteobacteria (Alph968) (Neef 1997), a new 16S rRNA-targeted oligonucleotide probe named S-O-Bac-0962-a-A-19 was designed. Its specificity was evaluated *in silico* by using the probeCheck (Loy *et al.* 2008) and Probe Match (Cole *et al.* 2014) tools. After hybridization and washing, the slides were rinsed in ice-cold deionized water, air-dried, and embedded in Citifluor AF1 (Citifluor, Hatfield, PA) antifading medium and observed under filter set 15 (Zeiss, Oberkochen, Germany) (546/12 nm excitation, 590 nm emission) with an Axio Imager Z.1 microscope equipped with an ApoTome system (Zeiss, Oberkochen, Germany).

Energy dispersive X-ray spectrometry

For EDXS analysis, calcium bodies from three specimens of each species were immersed in pure methanol upon dissection and embedded in Spurr's resin (SPI, West Chester, PA). Ultrathin sections were collected on holey-carbon-coated copper grids. Scanning transmission electron microscopy (STEM) imaging combined with EDXS analysis were performed using a VG HB501UX dedicated STEM operated in ultrahigh vacuum at an accelerating voltage of 100 kV, equipped with a cold field-emission gun (FEG) source and an EDXS system (Noran System SIX, Thermo Fisher Scientific, Waltham, MA). EDX maps and high-angle annular dark field-STEM images were obtained with a JEOL JEM-ARM200F (JEOL, Tokio, Japan) microscope, equipped with a cold FEG and a Quantax 200/S-STEM EDXS detector (Bruker, Bilerica, MA). Characteristic Ca-K and P-K X-ray lines were used for the quantification of Ca:P ratios. Quantitative EDX analysis has been done using experimentally determined k-factors measured from standard specimens under the same experimental conditions as for the measured samples.

RESULTS

16S rRNA gene sequence analysis

Four clone libraries comprising 172 bacterial 16S rRNA gene amplicons were constructed from the DNA isolates of the calcium bodies of two *Titanethes albus* and two *Hyloniscus riparius* individuals, while several attempts to amplify the archaeal 16S rRNA genes were unsuccessful. Cloned sequences were assigned to 12 OTUs, using the pairwise evolutionary distance threshold of 0.01. The 55 cloned sequences from Ta1 and 57 sequences from Ta2 clone library were assigned to seven OTUs each, while 30 sequences from Hr1 and 30 sequences from Hr2 clone libraries were assigned to three and four OTUs, respectively. Six OTUs shared the sequences obtained from both *T. albus* libraries (Ta1 and Ta2), while three OTU's shared the sequences from the clone libraries Hr1 and Hr2 obtained from the posterior calcium bodies of *H. riparius*.

Affiliation of the sequences in four clone libraries to higher taxa, percentage of shared nucleotide 7-mers (S˙ab score) with the nearest known sequences deposited in RDP database (Cole *et al.* 2014) and number of sequences in OTUs are given in Table 2.

Microscopic observations

Despite a considerable difference in the size of the calcium bodies in *T. albus* and *H. riparius*, the organs in both species exhibit

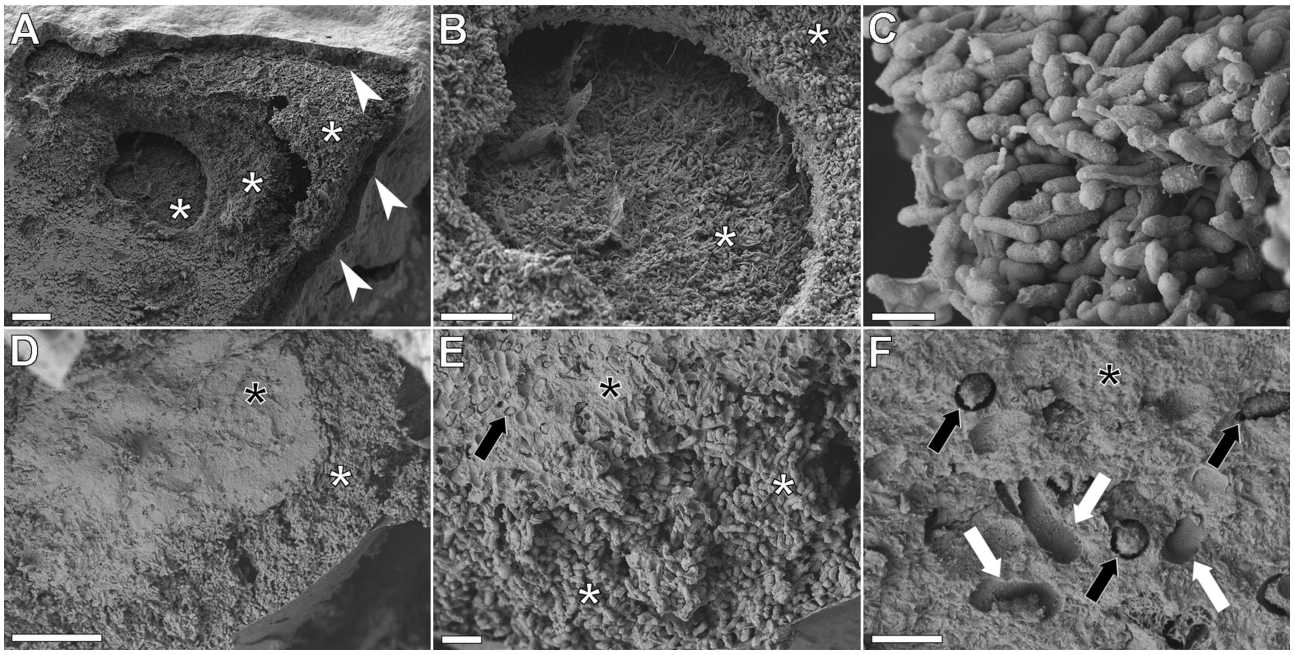

Figure 2. Scanning electron micrographs of bacteria-filled calcium bodies of *T. albus* (**A–C**) and *H. riparius* (**D–F**). (A) a fractured calcium body, showing the epithelial wall (arrowheads) on the surface of the structure and the bacteria-containing layers (white asterisks) in its contents. (**B**) Magnification of the calcium bodies center with numerous bacteria-containing layers (white asterisks). (C) Different bacterial morphotypes of bacteria-containing layers of calcium body. (D) A fractured calcium body showing the mineralized core (black asterisk) surrounded by bacteria-containing layers (white asterisks). (**E**) Magnification of the calcium body contents with numerous bacteria (white asterisk) surrounding the mineralized core with (black asterisk) with embedded bacteria (black arrows). (F) Bacterial casts (white arrows) and enclosed bacteria (black arrows) in the apatite mass (black asterisk) in the central area of calcium body. Scale bars: A and D—10 μm; B—5 μm; C and F—1 μm; E—2 μm.

similar anatomy (Fig. 2). The organs contain layers of dense bacterial formations (Fig. 2A, B, D and E) surrounding the core comprising bacteria embedded in a mineralized matrix (Fig. 2D–F) and overlaid by a single-layered epithelium on the surface of the organs (Fig. 2A). More detailed observation of the bacterial morphotypes in the posterior calcium bodies of *H. riparius* revealed the prevalence of non-flagellar rod-shaped bacteria, with slightly wrinkled surface throughout the calcium body (Fig. 2E and F). On the other hand, several bacterial morphotypes were observed in much larger calcium bodies of *T. albus*, including irregular, filamentous, helical and rod-shaped bacteria (Fig. 2C).

The observed diversity was further confirmed by TEM, which showed ultrastructural differences even within similar bacterial morphotypes (Fig. 3A, C and D). These include the density of bacterial cytoplasm and various cytoplasmic inclusions, among which electron-dense granules were the most frequently observed ultrastructural feature of the bacteria in the calcium bodies of both species (Fig. 3B and D). In addition, fission of the bacteria with cytoplasmic inclusions was observed in the ultrathin sections of the calcium bodies of both species (Fig. 3B and D)

Energy dispersive X-ray spectrometry

EDXS was performed on electron dense granules in the cytoplasm of methanol-fixed bacteria in the calcium bodies of *T. albus* and the posterior calcium bodies of *H. riparius*. EDX spectra of the granules feature prominent peaks of C, O, P and Ca (Fig. 4), with the ratio between Ca and P in the bacterial granules being 0.75 ± 0.08 in *T. albus* and 0.6 ± 0.009 in *H. riparius*. Such a composition and ratio between Ca and P is characteristic of bacterial intracellular polyphosphate granules, in which high amounts of metals such as Ca are often detectable in addition to P (Liu *et al.* 2001). By contrast, the P and Ca signals in spectra from other parts of the bacterial cytoplasm were much weaker (Fig. S1, Supporting Information).

DAPI staining and fluorescence *in situ* hybridization

The presence and distribution of polyphosphate-containing bacteria in the calcium bodies was shown by histochemical reaction based on fluorescence of polyphosphates after DAPI staining. DNA-specific light blue signal was observed in the epithelium and the lumen of the calcium bodies as well as other organs in the body cavity, while a strong and stable yellow fluorescence was limited to colonized parts of the calcium bodies of both species (Figs 5–7).

Hybridization by class-specific fluorescent probes (Table 1) confirmed the presence of Bacteroidetes and Alphaproteobacteria in the calcium bodies of *T. albus* (Fig. 6), and Bacteroidetes, Alphaproteobacteria and Betaproteobacteria in *H. riparius* (Fig. 7). This provides further evidence on the heterogeneous composition of the bacterial community of these organs. The uneven hybridization signals of individual probes revealed heterogeneous spatial distribution of the examined bacterial classes within the bacterial community, containing regions colonized by several bacterial classes as well as regions dominated by a single bacterial class (Fig. 6).

The polyphosphate-accumulating ability of the bacterial groups colonizing the calcium bodies was confirmed by DAPI staining of histological sections hybridized by class-specific probes. Partial overlapping of the yellow signal of the polyphosphates and class-specific red signals (Figs 6 and 7) confirmed the polyphosphate-accumulating ability among the

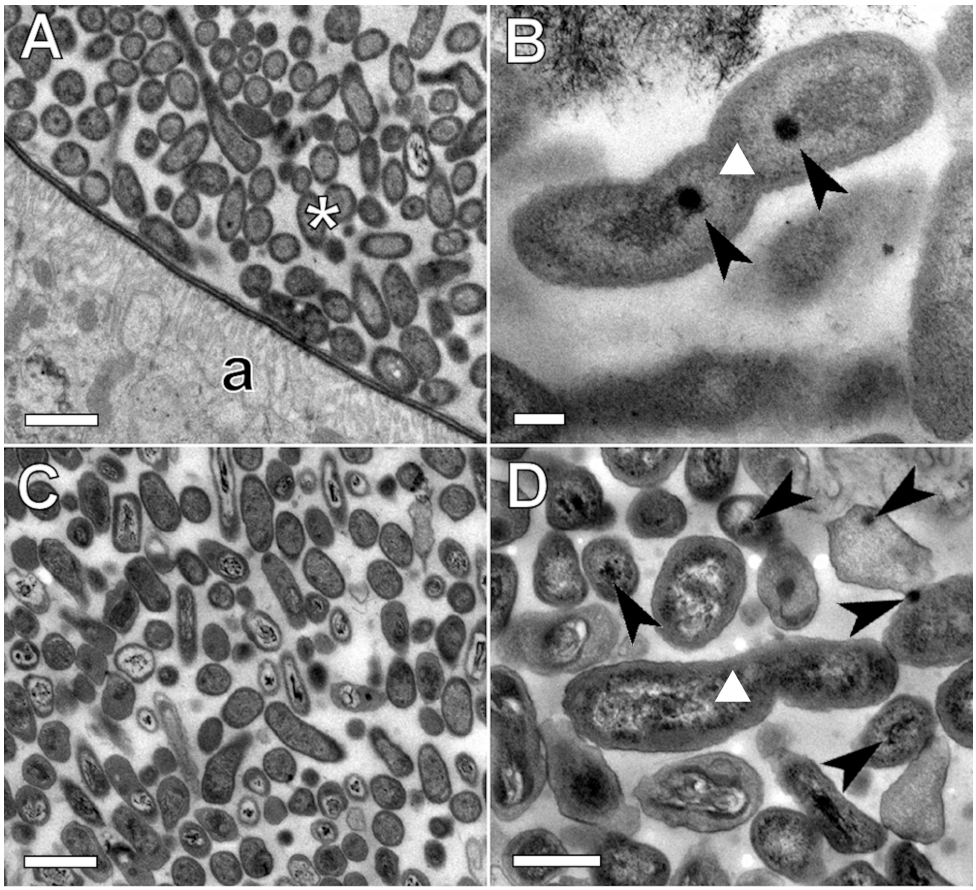

Figure 3. Transmission electron micrographs of bacteria in the calcium bodies of *H. riparius* (**A**, **B**) and *T. albus* (**C**, **D**). (A and C) diverse bacteria in the calcium bodies (white asterisk) above the apical surface (a) of the epithelium covering the organs. (B and D) diverse calcium bodies bacteria containing electron-dense cytoplasmic granules (arrowheads) and undergoing fission (white triangle). Scale bars: A and C—1 μm; B—200 nm; D—500 nm.

representatives of bacterial classes detected in the calcium bodies of each species by the 16S rRNA analysis.

DISCUSSION

As the first step towards illuminating the nature of the association and the role of each partner in this symbiosis, we described the composition of the bacterial community in the calcium bodies of two *Titanethes albus* and two *Hyloniscus riparius* individuals based on 16S rRNA gene sequence analysis. Successful amplification of bacterial 16S rRNA genes in both species and absence of the amplicons of archaeal rRNA genes in the initial step of construction of the clone libraries are concordant with previous results of domain-level *in situ* hybridization, which showed the prevalence of bacteria in these organs (Vittori *et al.* 2012).

The application of class-specific oligonucleotide probes in fluorescence *in situ* hybridization (FISH) performed on the tissue sections of the calcium bodies provide additional evidence on the coverage of the clone libraries in both isopod species and enabled insight into the abundance and the spatial organization of the bacteria in these organs. In accordance with the microscopic observations, FISH analysis confirmed the prevalence of a heterogeneous bacterial community throughout the lumen of the calcium bodies, comprising Bacteroidetes and Alphaproteobacteria in *T. albus* and Bacteroidetes, Alphaproteobacteria and Betaproteobacteria in *H. riparius*. Occasional regions colonized by single bacterial class were observed in both species.

Close affiliation of bacterial phylotypes in the calcium bodies to soil bacteria indicate colonization of these organs via a direct contact to the outer environment, similar to colonization of the digestive system in the isopod *Porcellio scaber* (Wang, Brune and Zimmer 2007; Horvathova, Kozlowski and Bauchinger 2015). Although the direct connection between the lumen of calcium bodies and the gut or the outer surface has not been shown in adult animals (Vittori *et al.* 2012, 2013), the presence of such connections in earlier stages of the ontogenetic development cannot be excluded. Besides, a fair permeability of the isopod's tissues to environmental bacteria and their dissemination between the tissues via the hemolymph was indicated in *Armadillidium Vulgare* (Bouchon, Zimmer and Dittmer 2016; Dittmer *et al.* 2016). Although microscopic observations, FISH analysis and DAPI staining of the tissues and organs surrounding the calcium bodies in our study did not confirm the bacterial presence, the suggested route may provide yet another conceivable strategy of colonization of the calcium bodies by the bacteria from outer environment. Regardless of their origin, the observed density of the bacteria in the calcium bodies clearly indicates their exploitation of the niche, while their close affiliation to ubiquitous soil taxa suggests a non-obligate nature of this association for the symbiont.

Although direct comparison of bacterial diversity between the calcium bodies and other colonized organs of terrestrial isopods might be influenced by sample size and methodological approach, the previously observed bacterial diversity in hemolymph, gonads and nerve cord of *A. vulgare* (Dittmer *et al.*

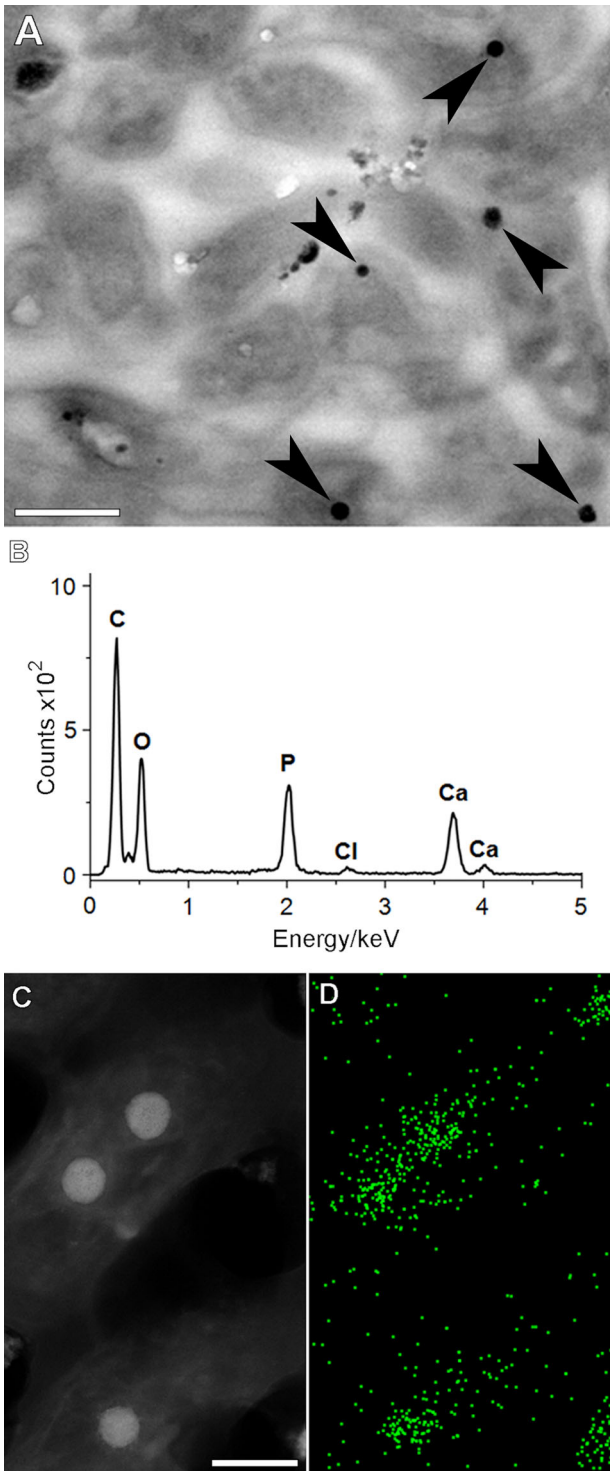

Figure 4. EDX analysis of polyphosphate granules within the bacterial cytoplasm. (**A**) Bright field STEM image of sectioned bacteria in *T. albus* calcium bodies. Electron dense granules (arrowheads) are visible in the bacterial cytoplasm. (**B**) EDX spectrum obtained from an electron dense granule in a *T. albus* calcium body, showing strong peaks of C, P, O and Ca, consistent with a polyphosphate. (**C**) High-angle annular dark-field STEM image of sectioned bacteria in *H. riparius* calcium bodies. Large polyphosphate granules are visible in the bacterial cytoplasm. (D) Map of P distribution in the area shown in C, demonstrating that the P signal is highly localized to the electron dense granules. Scale bars: A—1 μm; C—200 nm.

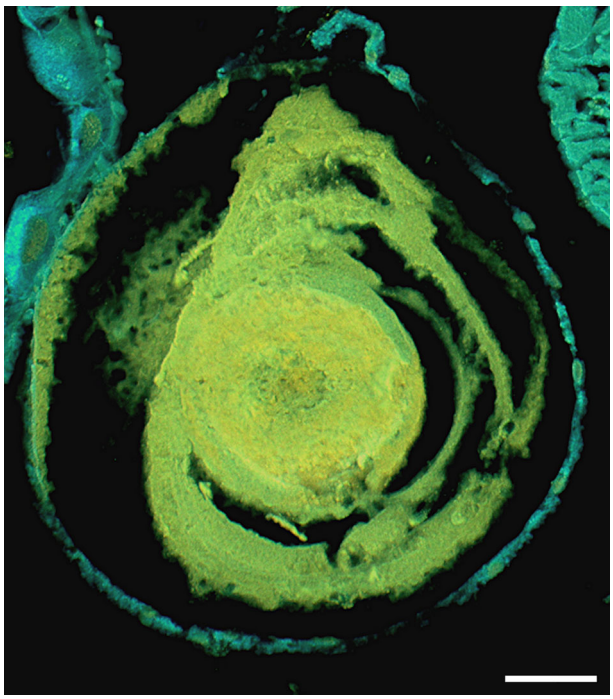

Figure 5. Yellow-green fluorescence in cross section of calcium body stained with DAPI indicating the presence of polyphosphate in the bacteria-containing layers and the core of calcium body. Scale bar: 50 μm.

2016) still fairly exceeds the number of observed OTUs in the calcium bodies. Despite lower diversity, the bacterial density in the calcium bodies observed by electron microscopy exceeds the bacterial concentrations in other colonized organs of terrestrial isopods, including the digestive system (Wang *et al.* 2004a,b; Kostanjšek *et al.* 2006; Dittmer *et al.* 2014). In view of high bacterial density localized to a particular organ, the calcium bodies may even exhibit certain morphological resemblance to insect bacteriomes housing obligate nutritional symbionts (Moran and Telang 1998; Baumann 2005). However, while the bacteria in the calcium bodies colonize the extracellular matrix in the lumen of the organ, the endosymbiotic bacteria of bacteriomes are commonly located in specialized cells, known as bacteriocytes (Douglas 1989). These provide nutrients and shelter to the endosymbiotic bacteria, which in exchange provide essential metabolites to the host (Douglas 1998). The bacteria in the calcium bodies are also more diverse compared to the bacteriomes, in which a constantly present and obligate 'primary symbiont' is only occasionally accompanied by other bacterial species or 'secondary symbionts' (Dale and Moran 2006). Primary symbionts generally belong to distinct and deeply branched phylogenetic lineages that coevolved with the host (Baumann 2005), while all bacteria in the calcium bodies exhibit close similarity to known bacterial taxa and clones isolated from the soil (Willems, Maergaret and Swings 2005; An *et al.* 2007; Hayat *et al.* 2010; Zhang *et al.* 2010; Maynaud *et al.* 2012).

Microbial symbiosis based on exchange of metabolites for shelter within the host tissues usually involves homogenous bacterial populations or complex microbial communities with common metabolic pathways or products (Douglas 1989; Baumann 2005; Kaltenpoth and Engl 2013). Although the possibility of similar symbiosis in the calcium bodies seemed less likely due to diversity and affiliation of the analyzed sequences to soil bacteria, the EDXS elemental analysis revealed the

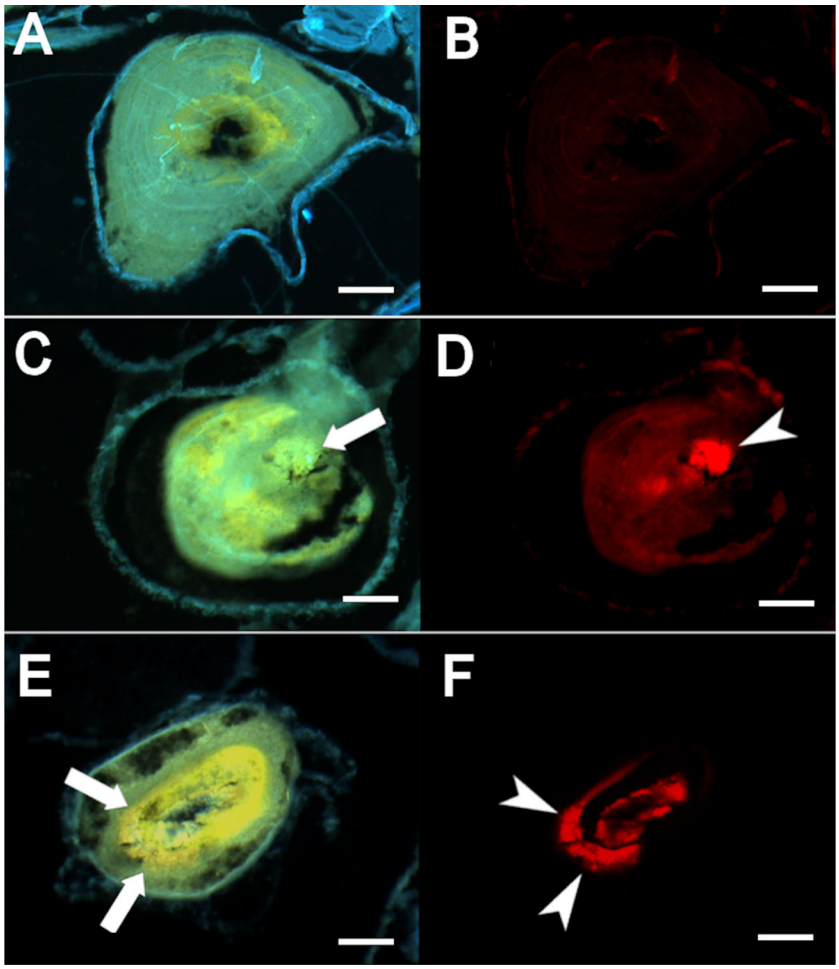

Figure 6. DAPI staining (**A**, **C**, **E**) of the *in situ* hybridized (**B**, **D**, **F**) calcium bodies of *T. albus*. (A and B) DAPI staining of the tissue section hybridized by the NON-338 probe (B), showing the background signal. (C and D) Overlapping of the polyphosphate-specific yellow signals (arrows) (C) and strong Alphaproteobacteria-specific signal (arrowheads) after hybridization with the Alph-968 probe (D). (E and F) Partial overlapping of the polyphosphate-specific yellow signal (arrows) (E) and strong Bacteroidetes-specific signal (arrowheads) after hybridization with the S-O-Bac-0962-a-A-19 probe (F). Scale bars: 50 μm.

presence of electron-dense cytoplasmic granules containing polyP as a prevailing ultrastructural feature of bacteria colonizing the calcium bodies. To analyze the distribution of the polyP in the calcium bodies and relate its presence to bacterial classes detected in these organs by 16S rRNA gene analysis, we used the combination of FISH analysis and histochemical analysis based on yellow fluorescence of polyP after DAPI staining (Allan and Miller 1980; Ruiz, Rodrigues and Docampo 2001; Pavlov *et al.* 2010). However, the emission of yellow fluorescent signal after staining with DAPI is not exclusively specific for polyP and may result from the presence of other negatively charged molecules, like inositol phosphate, heparin (Kolozsvari, Parisi and Saiardi 2014) and amorphous calcium phosphate (Omelon, Georgiou and Habraken 2016). While the presence of larger amounts of the former two in the calcium bodies was not expected, the amorphous calcium phosphate is known to occur in these organs (Vittori *et al.* 2012). The possibility of calcium phosphate being the source of yellow fluorescence signal in the calcium bodies has been significantly reduced by decalcification of our samples subjected to light microscopy and by the elemental analysis by EDXS. The latter confirmed that bacterial granules in the calcium bodies of both species contain Ca and P in ratios characteristic of polyphosphate (Doonan *et al.* 1979; Ashford *et al.* 1986), while the presence of calcium phosphates, characterized by much higher Ca to P ratios as observed (Wopenka and Pasteris 2005), was excluded.

FISH analysis linked the polyP-accumulating ability to all bacterial classes detected in the calcium bodies and considerably reduced the possibility of restriction of the polyP-accumulating ability to single bacterial taxon. The polyP-accumulating ability of the bacteria inhabiting the calcium bodies has been further supported by previous descriptions of the presence of polyphosphate kinase (Kornberg, Rao and Ault-Riche 1999) or cytoplasmic polyP granules in the taxa with the highest similarity to the phylotypes obtained from the calcium bodies. These include genera *Chitinophaga* [ACU58911] (Del Rio *et al.* 2010), *Sphingobacterium* [WP013663843], *Sphingopyxis* [ALH79362] (Ohtsubo *et al.* 2015), *Rhizobium* [WP018327404], *Devosia* [WP049705541], *Aminobacter* [WP055978852], *Mesorhizobium* [EHH13093] (Hao *et al.* 2012), *Bradyrhizobium* sp. (Kuyendall 2005) and *Variovorax paradoxus* (Willems *et al.* 1991; Willems, Maergaret and Swings 2005) [WP021007049]. Based on the deduction from known properties of their closest phenotypically characterized relatives, other metabolic similarities between bacteria in the calcium bodies were reduced to chemoorganotrophic utilization of the carbohydrates.

The ability of the bacteria to accumulate polyP evolved several times independently since it is widespread in diverse

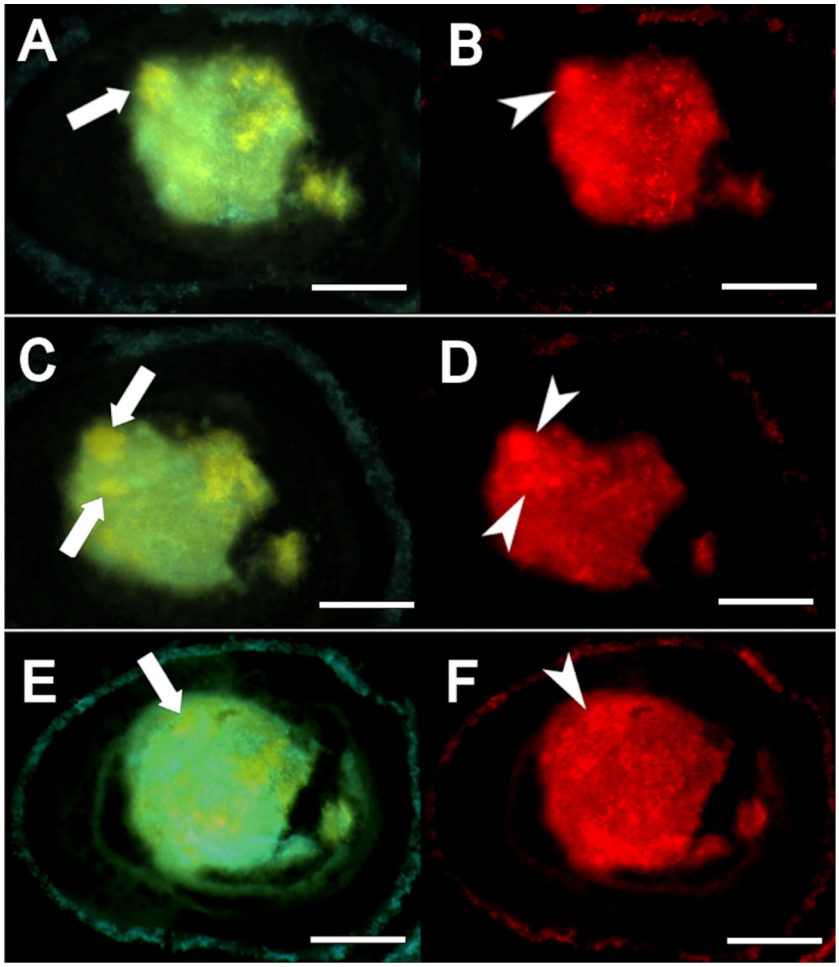

Figure 7. DAPI staining (**A**, **C**, **E**) of the *in situ* hybridized (**B**, **D**, **F**) calcium bodies of *H. riparius*. Overlapping of the polyphosphate-specific yellow signals (arrows) (A, C, E) and strong Alphaproteobacteria-specific signal (arrowheads) after hybridization with the Alph-968 probe (B), Betaproteobacteria-specific signal (arrowheads) after hybridization with the probe BET42a (D) and Bacteroidetes-specific signal (arrowheads) after hybridization with the S-O-Bac-0962-a-A-19 probe (F). Scale bars: 20 μm.

prokaryote taxa (Hirschler, Lucas and Hubert 1990). Despite the involvement of polyP in various processes in the bacterial cell, the main role of this polymer is considered to be the storage of phosphorus and energy in high-energy phosphorous bonds (Kornberg, Rao and Ault-Riche 1999). PolyP is reversibly polymerized by polyP kinase when sufficient amounts of phosphate and energy are available and depolymerized by phosphatases and other enzymes under conditions of energy or phosphorus deprivation (Hirschler, Lucas and Hubert 1990; Kornberg, Rao and Ault-Riche 1999). Thus, the presence of bacteria with polyP granules in the calcium bodies indicate the availability of phosphate and nutrients in the lumen of calcium bodies, which can be, as shown by the anatomy of the calcium bodies, delivered to the lumen only by transepithelial transport. At the same time, the presence of calcium phosphate in the colonized posterior calcium bodies and absence of phosphorus in the bacteria-free anterior pair of these organs in *H. riparius* strongly indicate the release of phosphate from polyP accumulated in bacterial symbionts (Vittori *et al.* 2013). As polymerization and hydrolysis of polyP cannot occur simultaneously, the most likely explanation for both processes would be the fluctuations of the available nutrients in the lumen. Regarding the described calcium dynamics in the calcium bodies during the molting cycle (Vittori *et al.* 2012), the formation of the glassy layer would be the most likely factor limiting the diffusion of the nutrients between the epithelium and bacteria inhabiting the lumen (Fig. 8). The bacteria would therefore store the energy by formation of polyP during absence of the glassy layer, and then, after the formation of this layer, recycle the stored energy in polyP under conditions of limited nutrient diffusion. According to the model we present here, the cyclic deprivation of nutrients might also constitute selective pressures favoring bacteria with efficient energy-storage capabilities, which would eventually result in the observed prevalence of the polyP-accumulating bacteria in the calcium bodies.

The bacteria present in the core of the calcium bodies are the most affected by limited nutrient diffusion through the epithelium covering the organs. Consequently, the bacteria in the core are forced to hydrolyze larger amounts of polyP to fulfill their energetic needs, comparing to the bacteria positioned closer to the epithelium. Increased concentrations of released inorganic phosphate in the core of the calcium bodies most likely provide the required amount of phosphate for the synthesis of apatite. Inorganic phosphate is, despite large amounts of calcium, the limiting factor for apatite precipitation in other parts of the calcium bodies (Omelon and Grynpas 2008; Omelon *et al.* 2014). As one of the most stable forms of calcium phosphate at neutral pH, the apatite gradually accumulates around the bacteria in the central region of the calcium body, forming the stable mineralized core of the organ (Vittori *et al.* 2012). Despite recently

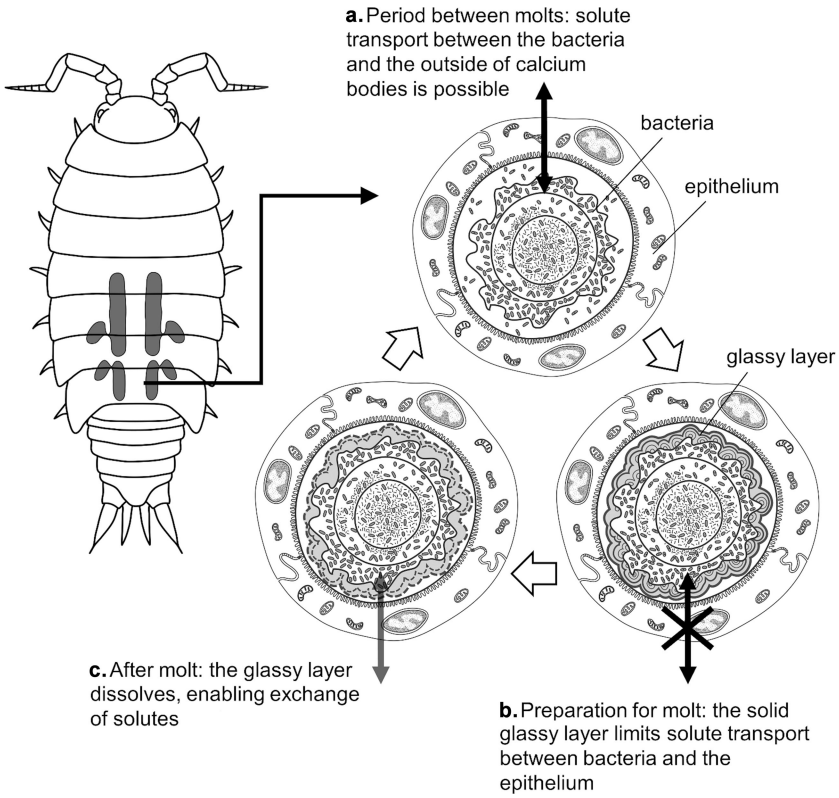

Figure 8. A schematic representation of the proposed model of changes affecting the bacterial population in the calcium bodies during a molting cycle. In non-molting individuals (**a**), solute transport between bacteria in the calcium bodies and the calcium body epithelium is unhindered, allowing the accumulation of polyphosphate by the bacterial cells. During preparation for molt (i.e. during late premolt stage) (**b**), the diffusion is limited by a glassy layer of calcium phosphate and calcium carbonate forming around the bacteria. As the bacterial population starves, it may resort to accumulated polyphosphate in their cytoplasm as a source of metabolic energy, releasing phosphate ions. After molt (**c**), the glassy layer dissolves, re-establishing solute transport between bacteria and the epithelium. As this occurs, the released phosphate ions may become available to the host.

suggested involvement of polyP in intracellular sequestration of calcium and biomineralizaion in unicellular marine algae (Sviben *et al.* 2016), the intracellular mineralization has not been observed in the polyP-accumulating bacteria in the calcium bodies.

The consequences of the symbiosis for the isopod host, on the other hand are not so unambiguous. Absence of pathogenesis and presence of dense bacterial population with common metabolic feature in specialized organs provide circumstantial evidence of isopod's adaptation to these symbionts. Soil bacteria were also recognized as a source of mutualistic symbiosis providing common metabolite to arthropod hosts (Kaltenpoth 2009). However, the costs and benefits of interaction between the isopod and symbionts in the calcium bodies are not clear. As the phosphate ions are an important component of the calcified exoskeleton and represent approximately 10% of the cuticle's dry weight in *T. albus* (Hild *et al.* 2009), the utilization of the phosphate released by symbionts in cyclic regeneration of the cuticle would be one of the likely benefits for the host from the symbiosis.

Most of the phosphate deposited in the isopod exoskeleton is located in the endocuticle, the cuticle layer which forms in the postmolt stage of the molting cycle (Hild *et al.* 2009). The need for phosphate used in the endocuticle deposition therefore coincides with the disintegration of the glassy layer surrounding the bacteria in the core of the calcium bodies (Vittori *et al.* 2012). In accordance with the postulated model of phosphate dynamics in the calcium bodies, it is plausible that removal of the glassy layer facilitates the diffusion of the phosphate accumulated in the core during symbiotic hydrolysis of polyP to the tissues and therefore enables its sequestration by newly forming endocuticle. In contrast to the polyP-accumulating bacterial community in marine sponges, which provide the phosphorus sequestered from the filtered sea water to the host (Zhang *et al.* 2015), the phosphate accumulated in the symbionts of the calcium bodies originates from the isopod's tissues and excludes the host's dependence on polyP-accumulating bacteria in the process of the calcium storage and recycling.

The presence of calcium bodies has been demonstrated in numerous other trichoniscids, including the genera *Alpioniscus*, *Androniscus*, *Calconiscellus*, *Haplophthalmus* and *Trichoniscus* (Verhoeff 1926, 1927; Méhelÿ 1932; Vittori and Štrus 2016). Bacteria have been demonstrated within these organs in all species studied ultrastructurally, namely in *T. albus*, *H. riparius*, *Androniscus roseus*, and *Haplophthalmus mengei* (Vittori *et al.* 2012, 2013; Vittori and Štrus 2016). However, such structures are not known outside trichonscids and further work is necessary to establish in which oniscidean lineages they occur.

In conclusion, the symbiosis described here appears to be non-obligate for both host and symbionts. The latter apparently exploits the niche within the calcium bodies, while the benefit for the host is much more ambiguous and, if present, most likely includes the utilization of the phosphate released by the symbionts in exoskeleton formation. Further experiments, as well as comprehensive anatomical studies at earlier developmental stages, are required to elucidate the routes of primary colonization of calcium bodies as well as the exact costs and benefits of the this unique association, which, to our knowledge,

represents the first evidence on polyP-accumulating bacterial symbionts in the tissue of a terrestrial animal.

SUPPLEMENTARY DATA

Supplementary data are available at *FEMSEC* online.

ACKNOWLEDGEMENTS

We thank Birgit Bussmann from the Stuttgart Center for Electron Microscopy, Max Planck Institute for Solid State Research, for the TEM specimen preparation, Dr Andrej Blejec from National Institute of Biology, Ljubljana, for constructive suggestions on data presentation and Dr. Stanley K. Sessions from Hartwick College for proofreading and constructive remarks on the manuscript.

FUNDING

This work was supported by the European Union Seventh Framework Program under Grant Agreement 312483—ESTEEM2 (Integrated Infrastructure Initiative—I3) and by the Slovenian Research Agency (ARRS) research program P1-0148.

Conflict of interest. None declared.

REFERENCES

Allan RA, Miller JJ. Influence of s-adenosylmethionine on dapi-induced fluorescence of polyphosphate in the yeast vacuole. *Can J Microbiol* 1980;**26**:912–20.

An D-S, Im W-T, Lee S-TK *et al. Chitinophaga soli* sp. nov. and *Chitinophaga terrae* sp. nov. isolated from soil of a ginseng field in Pocheon Province, Korea. *J Microbiol Biotechn* 2007;**17**:705–11.

Aschar-Sobbi R, Abramov AY, Diao C *et al.* High sensitivity, quantitative measurements of polyphosphate using a new DAPI-Based approach. *J Fluoresc* 2008;**18**:859–66.

Ashford AE, Peterson RL, Dwarte D *et al.* Polyphosphate granules in eucalypt mycorrhizas - determination by energy dispersive-x-ray microanalysis. *Can J Bot* 1986;**64**:677–87.

Baumann P. Biology of bacteriocyte-associated endosymbionts of plant sap-sucking insects. *Annu Rev Microbiol* 2005;**59**:155–89.

Becker A, Bismayer U, Epple M *et al.* Structural characterisation of X-ray amorphous calcium carbonate (ACC) in sternal deposits of the crustacea *Porcellio scaber*. *Dalton T* 2003, DOI 10.1039/b210529b:551-5.

Bouchon D, Zimmer M, Dittmer J. The terrestrial isopod microbiome: an all-in-one toolbox for animal-microbe interactions of ecological relevance. *Front Microbiol* 2016;**7**:1472.

Cole JR, Wang Q, Fish JA *et al.* Ribosomal database project: data and tools for high throughput rRNA analysis. *Nucleic Acids Res* 2014;**42**:D633–42.

Cordaux R, Paces-Fessy M, Raimond M *et al.* Molecular characterization and evolution of arthropod-pathogenic *Rickettsiella* bacteria. *Appl Environ Microb* 2007;**73**:5045–7.

Daims H, Stoecker K, Wagner M. Fluoresence in situ hybridization for detection of prokaryotes. In: Osborn AM, Smith CJ (eds). *Molecular Microbial Ecology*. New York: Taylor & Francis Group, 2005, 213–39.

Dale C, Moran NA. Molecular interactions between bacterial symbionts and their hosts. *Cell* 2006;**126**:453–65.

Del Rio TG, Abt B, Spring S *et al.* Complete genome sequence of Chitinophaga pinensis type strain (UQM 2034(T)). *Stand Genomic Sci* 2010;**2**:87–95.

DeLong EF. Archaea in coastal marine environments. *P Natl Acad Sci USA* 1992;**89**:5685–9.

Dittmer J, Beltran-Bech S, Lesobre J *et al.* Host tissues as microhabitats for *Wolbachia* and quantitative insights into the bacterial community in terrestrial isopods. *Mol Ecol* 2014;**23**:2619–35.

Dittmer J, Lesobre J, Moumen B *et al.* Host origin and tissue microhabitat shaping the microbiota of the terrestrial isopod *Armadillidium vulgare*. *FEMS Microbiol Ecol* 2016;**92**, DOI: 10.1093/femsec/fiw063.

Doonan BB, Crang RE, Jensen TE *et al.* In situ X-ray energy dispersive microanalysis of polyphosphate bodies in *Aureobasidium pullulans*. *J Ultrastruc Res* 1979;**69**:232–8.

Douglas AE. Mycetocyte symbiosis in insects. *Biol Rev Camb Philos* 1989;**64**:409–34.

Douglas AE. Nutritional interactions in insect-microbial symbioses: aphids and their symbiotic bacteria *Buchnera*. *Annu Rev Entomol* 1998;**43**:17–37.

Edgar RC. MUSCLE: multiple sequence alignment with high accuracy and high throughput. *Nucleic Acids Res* 2004;**32**:1792–7.

Fraune S, Zimmer M. Host-specificity of environmentally transmitted *Mycoplasma*-like isopod symbionts. *Environ Microbiol* 2008;**10**:2497–504.

Günther S, Trutnau M, Kleinsteuber S *et al.* Dynamics of polyphosphate-accumulating bacteria in wastewater treatment plant microbial communities detected via DAPI (4′,6′-Diamidino-2-Phenylindole) and tetracycline labeling. *Appl Environ Microb* 2009;**75**:2111–21.

Hao X, Lin Y, Johnstone L *et al.* Draft genome sequence of plant growth-promoting rhizobium *Mesorhizobium amorphae*, isolated from zinc-lead mine tailings. *J Bacteriol* 2012;**194**:736–7.

Hayat R, Ali S, Amara U *et al.* Soil beneficial bacteria and their role in plant growth promotion: a review. *Ann Microbiol* 2010;**60**:579–98.

Hild S, Neues F, Znidarsic N *et al.* Ultrastructure and mineral distribution in the tergal cuticle of the terrestrial isopod *Titanethes albus*. Adaptations to a karst cave biotope. *J Struct Biol* 2009;**168**:426–36.

Hirschler A, Lucas J, Hubert JC. Bacterial involvement in apatite genesis. *FEMS Microbiol Ecol* 1990;**73**:211–20.

Hornung E. Evolutionary adaptation of oniscidean isopods to terrestrial life: structure, physiology and behavior. *Terr Arthropod Rev* 2011;**4**:95–130.

Horvathova T, Babik W, Bauchinger U. Biofilm feeding: microbial colonization of food promotes the growth of a detritivorous arthropod. *Zookeys* 2016, DOI 10.3897/zookeys.577.6149:25-41.

Horvathova T, Kozlowski J, Bauchinger U. Growth rate and survival of terrestrial isopods is related to possibility to acquire symbionts. *Eur J Soil Biol* 2015;**69**:52–6.

Kaltenpoth M. Actinobacteria as mutualists: general healthcare for insects? *Trends Microbiol* 2009;**17**:529–35.

Kaltenpoth M, Engl T. Defensive microbial symbionts in Hymenoptera. *Funct Ecol* 2013;**28**:315–27.

Kim M, Oh H-S, Park S-C *et al.* Towards a taxonomic coherence between average nucleotide identity and 16S rRNA gene sequence similarity for species demarcation of prokaryotes. *Int J Syst Evol Micr* 2014;**64**:346–51.

Kolozsvari B, Parisi F, Saiardi A. Inositol phosphates induce DAPI fluorescence shift. *Biochem J* 2014;**460**:377–85.

Kornberg A, Rao NN, Ault-Riche D. Inorganic polyphosphate: a molecule of many functions. *Annu Rev Biochem* 1999;**68**:89–125.

Kostanjsek R, Pasic L, Daims H *et al.* Structure and community composition of sprout-like bacterial aggregates in

a Dinaric karst subterranean stream. *Microb Ecol* 2013; **66**:5–18.

Kostanjsek R, Strus J, Avgustin G. "*Candidatus* Bacilloplasma," a novel lineage of Mollicutes associated with the hindgut wall of the terrestrial isopod *Porcellio scaber* (Crustacea: Isopoda). *Appl Environ Microb* 2007;**73**:5566–73.

Kostanjsek R, Strus J, Drobne D *et al.* '*Candidatus* Rhabdochlamydia porcellionis', an intracellular bacterium from the hepatopancreas of the terrestrial isopod *Porcellio scaber* (Crustacea: Isopoda). *Int J Syst Evol Micr* 2004;**54**:543–9.

Kostanjšek R, Štrus J, Lapanje A *et al.* Intestinal microbiota of terrestrial isopods. In: Konig H, Varma, A (eds). *Intestinal Microorganisms of Termites and Other Invertebrates*, Vol. 6. Berlin: Springer-Verlag, 2006, 115–31.

Kuyendall LD. Genus I. *Bradyrhizobium*. In: Brenner DJ, Krieg NR, Staley JT (eds). *Bergey's Manual of Systematic Bacteriology. Volume 2. The Proteobacteria, Part C: the Alpha-, Beta-, Delta-, and Epsilonproteobacteria*. 2nd edn. New York: Springer, 2005, 438–43.

Liu WT, Nielsen AT, Wu JH *et al.* In situ identification of polyphosphate- and polyhydroxyalkanoate-accumulating traits for microbial populations in a biological phosphorus removal process. *Environ Microbiol* 2001;**3**:110–22.

Loy A, Arnold R, Tischler P *et al.* probeCheck - a central resource for evaluating oligonucleotide probe coverage and specificity. *Environ Microbiol* 2008;**10**:2894–8.

Manz W, Amann R, Ludwig W *et al.* Phylogenetic oligodeoxynucleotide probes for the major subclasses of proteobacteria - problems and solutions. *Syst Appl Microbiol* 1992;**15**:593–600.

Maynaud G, Willems A, Soussou S *et al.* Molecular and phenotypic characterization of strains nodulating *Anthyllis vulneraria* in mine tailings, and proposal of *Aminobacter anthyllidis* sp. nov. the first definition of *Aminobacter* as legume-nodulating bacteria. *Syst Appl Microbiol* 2012;**35**:65–72.

Méhelÿ LV. Beiträge zur anatomie der trichonisciden. *Stud Zool Regiae Sci Univ Hung Budapestensis Fundatae a Petro Pazmany* 1932;**2**:83–119.

Moran NA, Telang A. Bacteriocyte-associated symbionts of insects - A variety of insect groups harbor ancient prokaryotic endosymbionts. *Bioscience* 1998;**48**:295–304.

Neef A. *Anwendung der in situ Einzelzell-Identifizierung von Bakterien zur Populationsanalyse in komplexen mikrobiellen Biozönosen*. München: Technische Universität München, 1997, 141.

Ohtsubo Y, Nagata Y, Numata M *et al.* Complete genome sequence of polypropylene glycol- and polyethylene glycol-degrading *Sphingopyxis macrogoltabida* strain EY-1. *Genome Announc* 2015;**3**:e01399–15.

Omelon S, Georgiou J, Habraken W. A cautionary (spectral) tail: red-shifted fluorescence by DAPI-DAPI interactions. *Biochem Soc T* 2016;**44**:46–9.

Omelon S, Georgiou J, Variola F *et al.* Colocation and role of polyphosphates and alkaline phosphatase in apatite biomineralization of elasmobranch tesserae. *Acta Biomater* 2014;**10**:3899–910.

Omelon SJ, Grynpas MD. Relationships between polyphosphate chemistry, biochemistry and apatite biomineralization. *Chem Rev* 2008;**108**:4694–715.

Pavlov E, Aschar-Sobbi R, Campanella M *et al.* Inorganic polyphosphate and energy metabolism in mammalian cells. *J Biol Chem* 2010;**285**:9420–8.

Ruiz FA, Rodrigues CO, Docampo R. Rapid changes in polyphosphate content within acidocalcisomes in response to cell growth, differentiation, and environmental stress in *Trypanosoma cruzi*. *J Biol Chem* 2001;**276**:26114–21.

Schloss PD, Westcott SL, Ryabin T *et al.* Introducing mothur: open-source, platform-independent, community-supported software for describing and comparing microbial communities. *Appl Environ Microb* 2009;**75**:7537–41.

Sviben S, Gal A, Hood MA *et al.* A vacuole-like compartment concentrates a disordered calcium phase in a key coccolithophorid alga. *Nat Commun* 2016;**7**:11228.

Verhoeff KW. Isopoden der Balkanhalbinsel, gesammelt von Herrn D-r I. Buresch. Zugleich 31. Isopoden-Aufsatz. *Mitteilungen der Bulgarischen Entomologischen Gesellschaft in Sofia* 1926;**3**:135–58.

Verhoeff KW. *Illyrionethes* n. g. eine cavernicole Trichonisciden-Gattung. 35. Isopoden-Aufsatz. *Zool Anz* 1927;**72**:268–74.

Vittori M, Kostanjšek R, Žnidaršič N *et al.* Calcium bodies of *Titanethes albus* (Crustacea: Isopoda): molt-related structural dynamics and calcified matrix-associated bacteria. *J Struct Biol* 2012;**180**:216–25.

Vittori M, Rozman A, Grdadolnik J *et al.* Mineral deposition in bacteria-filled and bacteria-free calcium bodies in the crustacean *Hyloniscus riparius* (Isopoda: Oniscidea). *PLoS One* 2013;**8**:1–14.

Vittori M, Štrus J. The presence of bacteria in calcium bodies of the terrestrial isopods *Androniscus roseus* and *Haplophthalmus mengei*. *Acta Biol Slov* 2016;**59**:47–55.

Wallner G, Amann R, Beisker W. Optimizing fluorescent insitu hybridization with ribosomal-rna-targeted oligonucleotide probes for flow cytometric identification of microorganisms. *Cytometry* 1993;**14**:136–43.

Wang YJ, Brune A, Zimmer M. Bacterial symbionts in the hepatopancreas of isopods: diversity and environmental transmission. *FEMS Microbiol Ecol* 2007;**61**:141–52.

Wang YJ, Stingl U, Anton-Erxleben F *et al.* "Candidatus Hepatoplasma crinochetorum," a new, stalk-forming lineage of Mollicutes colonizing the midgut glands of a terrestrial isopod. *Appl Environ Microb* 2004a;**70**:6166–72.

Wang YJ, Stingl U, Anton-Erxleben F *et al.* 'Candidatus Hepatincola porcellionum' gen. nov. sp nov. a new, stalk-forming lineage of Rickettsiales colonizing the midgut glands of a terrestrial isopod. *Arch Microbiol* 2004b; **181**:299–304.

Warburg MR. Isopods and their terrestrial environment. In: Macfadyen A, Ford ED (eds). *Advances in Ecological Research*, Volume 17. London: Acadamic Press, 1987, 187–242.

Willems A, Deley J, Gillis M *et al. Comamonadaceae*, a new family encompassing the *Acidovorans* ribosomal-RNA complex, including *Variovorax paradoxus* gen. nov. comb. nov. for *Alcaligenes paradoxus* (Davis 1969). *Int J Syst Bacteriol* 1991;**41**:445–50.

Willems A, Maergaret J, Swings J. Genus X. *Variovorax*. In: Brenner DJ, Krieg NR, Staley JT (eds). *Bergey's manual of systematic bacteriology Volume 2: The Proteobacteria, part C : the Alpha-, Beta-, Delta-, and Epsilonproteobacteria*. 2nd edn. New York: Springer, 2005, 732–5.

Wopenka B, Pasteris JD. A mineralogical perspective on the apatite in bone. *Mat Sci Eng C* 2005;**25**:131–43.

Wright ES, Yilmaz LS, Noguera DR. DECIPHER, a search-based approach to chimera identification for 16S rRNA sequences. *Appl Environ Microb* 2012;**78**:717–25.

Zhang D-C, Liu H-C, Xin Y-H *et al. Sphingopyxis bauzanensis* sp. nov., a psychrophilic bacterium isolated from soil. *Int J Syst Evol Micr* 2010;**60**:2618–22.

Zhang F, Blasiak LC, Karolin JO *et al.* Phosphorus sequestration in the form of polyphosphate by microbial

symbionts in marine sponges. *P Natl Acad Sci USA* 2015; **112**:4381–6.

Ziegler A. Ultrastructural changes of the anterior and posterior sternal integument of the terrestrial isopod *Porcellio scaber* latr (Crustacea) during the moult cycle. *Tissue Cell* 1997;**29**:63–76.

Ziegler A. Calcium deposition and resorption in the sternal CaCO3 deposits of *Porcellio scaber* (Isopoda), ultrastructure and molecular mechanisms. *Bone* 2005;**36**:S466–66.

Ziegler A, Fabritius H, Hagedorn M. Microscopical and functional aspects of calcium-transport and deposition in terrestrial isopods. *Micron* 2005;**36**:137–53.

Ziegler A, Hagedorn M, Ahearn GA *et al*. Calcium translocations during the moulting cycle of the semiterrestrial isopod *Ligia hawaiensis* (Oniscidea, Crustacea). *J Comp Physiol B* 2007;**177**:99–108.

Zimmer M. Nutrition in terrestrial isopods (Isopoda: Oniscidea): an evolutionary-ecological approach. *Biol Rev* 2002;**77**:455–93.